Optimization for Error-Canceling Loop of the Feedforward Amplifier Using a New System-Level Mathematical Model

Youngoo Yang, *Member, IEEE*, Young Yun Woo, and Bumman Kim, *Senior Member, IEEE*

***Abstract*—We present a system-level mathematical model to simulate the linearity of the feedforward amplifier. The model has fundamental and distortion signal sub-paths constructed from the data extracted by baseband system simulation. The calculated linearization performances using the model have been validated by comparison with the baseband system simulation results. From the calculated results, the optimum design of the error amplifier size and coupling factor of the output coupler for a down-link WCDMA signal with 16 data channels are provided to maximally achieve output linearity with a fixed power capacity of the amplifiers. Our data shows that the optimum size of the error amplifier is 0.45 times that of the main amplifier with the coupling factor of 5.5 dB.**

***Index Terms*—Adjacent channel leakage ratio (ACLR), baseband system, feedforward amplifier, linearity, mathematical model, peak-to-average ratio, signal statistics, spectrum emission, WCDMA.**

I. Introduction

LINEAR amplification of the RF modulated signal is essential for most recent wireless communication systems. Many techniques, including feedforward, envelope feedback, manifold types of predistorters, etc., have been extensively used to effectively satisfy the specifications and costs for various system applications. Communication systems that utilize code division multiple access (CDMA), orthogonal frequency division multiplexing (OFDM) and so on use the modulated signals with complex signal statistics. The signal statistics, which are generally delegated by peak-to-average ratio, significantly affect the linearity of high power amplifiers and their linearizers [1]–[3]. Hence, signal statistics are among the most important considerations in linear power-amplifier design.

Among many linearization methods, feedforward is generally known as the best technique for RF power amplifiers with the highest improvement in linearity. Many previous works for various implementations and analyses of the feedforward-type linearizers have been reported [2]–[13]. To compensate for the low tolerance of linearization mechanism due to its subtraction nature, various types of analog or digital control circuits have been employed [3]–[5]. Explicit analyses for the cancellation tolerance, delay mismatch, loop instability, and efficiency have already been reported [6]–[13].

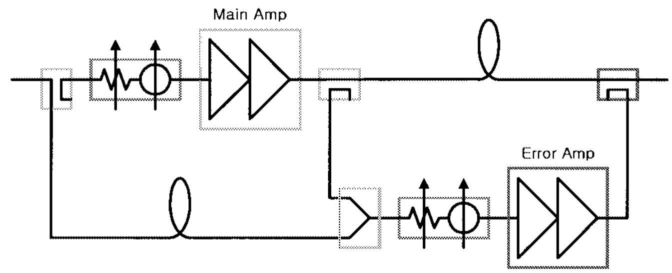

Fig. 1. Schematic diagram of the feedforward amplifier.

The basic schematic diagram of the feedforward amplifier is shown in Fig. 1. The amplifier has two cancellation loops. In the signal cancellation loop (or first loop), the subtraction of the input signal component from the coupled output signal of the main amplifier provides a pure error signal, which has totally different signal statistics from the main input signal. This error signal is adjusted by the vector modulator and amplified by the error amplifier to cancel the distortion component of the main amplifier output by direct subtraction using the output coupler in the error cancellation loop (or second loop).

It is known that the linearity enhancement of the feedforward amplifier is mainly limited by cancellation tolerance (i.e., amplitude and phase imbalances between the main and error signals), signal coupling between the main and error signals, and the nonideal effect of the couplers (i.e., finite directivity or isolation). As the peak-to-average ratio of input signal increases, however, saturation of the error amplifier at the peak power level becomes an important factor to restrict the performance of the feedforward amplifier. The distortion caused by saturation results in a very different linearization performance between the signals with two tones (generally reported for over 30-dB improvement) and a modulated signal having a high peak-to-average ratio (generally reported for around 15–25-dB improvement), such as CDMA, WCDMA, etc. Therefore, the behavior of the feedforward amplifier, especially of the error amplifier, as related to signal statistics is very important for linearization. Nevertheless, design considerations that include signal statistics have not yet been explicitly explained.

In this paper, a new design approach to optimize the second-loop parameters of the feedforward amplifiers for lin-

Manuscript received November 21, 2001. This work was supported in part by the Agency for Defense Development and by the Korean Ministry of Education under the Brain Korea 21 Project.

Y. Yang was with the Department of Electronic and Electrical Engineering, Pohang University of Science and Technology, Pohang 790-784, Korea. He is now with Skyworks Solutions Inc., Newbury Park, CA 91320 USA (e-mail: youngoo.yang@skyworksinc.com)

Y. Y. Woo and B. Kim are with the Department of Electronic and Electrical Engineering and the Microwave Application Research Center, Pohang University of Science and Technology, Pohang 790-784, Korea (e-mail: bmkim@postech.ac.kr).

Digital Object Identifier 10.1109/TMTT.2002.807824

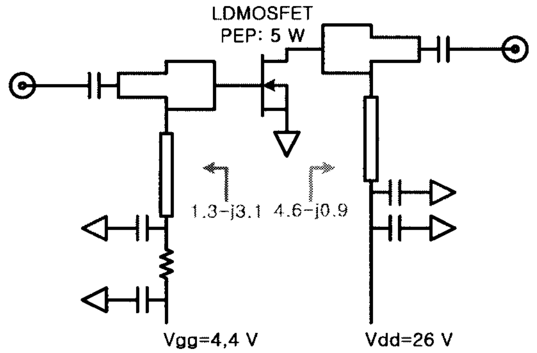

Fig. 2. Schematic diagram of the designed amplifier providing a basic amplifier cell for both the main and error amplifiers.

earity improvements is presented. We employ a mathematical model of the main and error amplifiers, which are suited to their different signal statistics for WCDMA signal. This simplified model saves the simulation and data collection time compared with the usual baseband signal simulation. From the simulation using the mathematical model, the size of the error amplifier and coupling factor of the output coupler are optimized for linearity improvement. For optimization, only the saturation effect of the error amplifier are included since it is the dominant degrading factor for linearization, as mentioned above. The data extraction and modeling procedure will also be described.

II. Mathematical Modeling

To build the mathematical model of a power amplifier, a baseband built-in amplifier model has been constructed and the mathematical model parameters are extracted from the baseband simulation. The RF power amplifier is designed by using harmonic-balance simulation in Agilent's ADS with a large-signal model of the 5-W peak envelope power (PEP) LD-MOSFET at 2.14 GHz. A schematic diagram of the designed amplifier, which is used as a basic amplifier cell for both the main and error amplifiers, is shown in Fig. 2. The designed amplifier is remodeled to a built-in baseband amplifier model with optimized parameters of the third-order intercept (TOI) point, 1-dB gain compression point (P1dB), saturated power (Psat), and gain compression at saturation (Gsat), i.e., to fit the one- and two-tone amplitude responses. This remodeling process saves simulation time to extract the mathematical model parameters.

The baseband modeling results are shown in Fig. 3. Fig. 3(a) shows the AM–AM responses of the amplifiers based on the large-signal model and baseband model. Fig. 3(b) shows the simulated two-tone characteristics, which are closely matched between the amplifiers based on the large-signal model and baseband model through a broad power range, including third-order intermodulation (IM3) terms, as well as fundamentals. The optimized parameters of the baseband amplifier model for the 5-W PEP 2.14-GHz amplifier are listed in Table I.

A. Mathematical Model Description

The main feature of the mathematical model is two separated paths for linear amplification and distortion generation and can handle the uncorrelated signals. The main and error amplifiers are also modeled differently because they are dealing with signals with far different statistics.

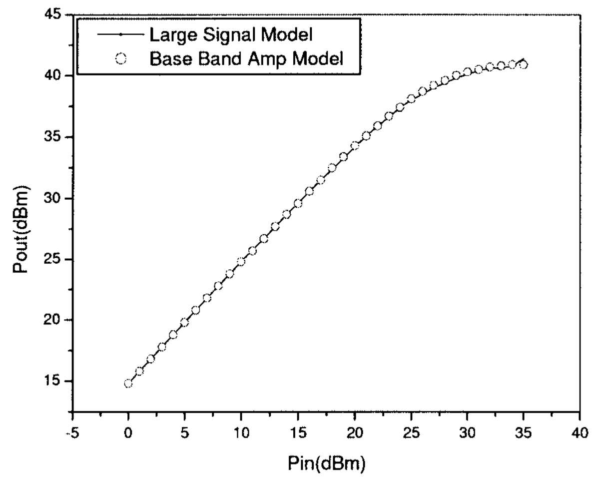

(a)

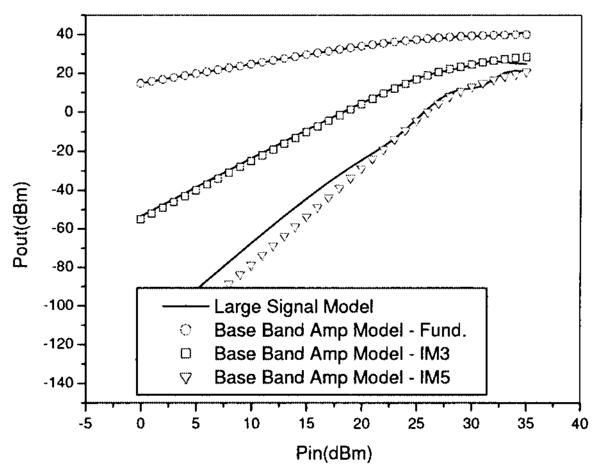

(b)

Fig. 3. (a) Simulated AM–AM responses. (b) Simulated two-tone characteristics of the amplifiers using the large-signal and optimized baseband models.

TABLE I
Optimized Parameters of the Baseband Amplifier Model for 5-W PEP 2.14-GHz Amplifier

param.	value	unit
Gain	14.8283	dB
TOI	46.7209	dBm
Psat	41.4027	dBm
P1dB	36.4027	dBm
Gsat	7.0	dB

The symbols of the mathematical model for the main and error amplifiers are visualized in Fig. 4. As shown, the models have one input, but have two separate outputs to handle the distortion terms uncorrelated to linear output. $L_{\rm MA}$ is the linear output term from the main amplifier, which is 100% correlated to the input signal drawn as a solid line. $L_{\rm MA}$ is an amplitude in dBm at the center frequency with 30-kHz resolution bandwidth. $D_{\rm MA}$ is shown as a short dashed line in this figure, and is the distortion term of the main amplifier, which is perfectly uncorrelated to the input signal. $D_{\rm MA}$ is an amplitude in dBm at an offset of 2.5 MHz from the center

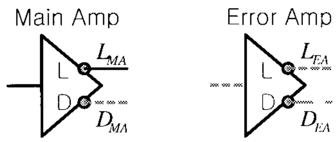

Fig. 4. Symbols used for the mathematical modeling of the main and error amplifiers.

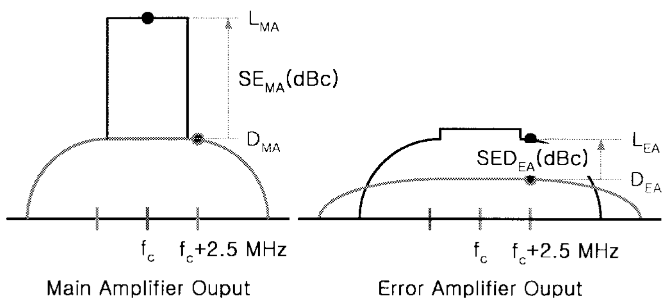

Fig. 5. Illustrations for the output power spectral densities of the main and error amplifiers and parameters used in the modeling.

frequency, with 30-kHz resolution bandwidth. This is the most important frequency for the spectrum emission specification for the third-generation WCDMA application since the signal statistics are not considerably changed by the number of carriers. The adjacent channel leakage ratio (ACLR) for the multicarrier signal is very closely coupled to the spectrum emission at offset 2.5 MHz for the single-carrier signal, which is an empirically accepted fact for high-power silicon LDMOSFET amplifier design. The signal definition for the error amplifier is somewhat different from that of the main amplifier because of the different error signal statistics. $L_{\rm EA}$ is also shown as a short dashed line in Fig. 4, and is the linear output term of the error amplifier. It is 100% correlated to the input signal of the error amplifier, and is the distortion component of the main amplifier. $D_{\rm EA}$ is shown as a long dashed line, and is the distortion term of the error amplifier, which is uncorrelated to the input signal of the error amplifier. $L_{\rm EA}$ and $D_{\rm EA}$ are defined in the same way as $D_{\rm MA}$.

The output power spectral densities for the main and error amplifiers are depicted in Fig. 5. $L_{\rm MA}$, $D_{\rm MA}$, $L_{\rm EA}$, and $D_{\rm EA}$ explained above are clearly indicated using spectral diagrams. From Fig. 5, the out-of-band spectrum emission at an offset of 2.5 MHz (abbreviated as $\rm SE_{MA}$) of the main amplifier and the out-of-band spectrum emission generated by the error amplifier (abbreviated as $\rm SED_{EA}$) are defined as

$$\mathrm{SE_{MA}} = D_{\rm MA} - L_{\rm MA} \text{ (dBc)} \tag{1}$$

$$\mathrm{SED_{EA}} = D_{\rm EA} - L_{\rm EA} \text{ (dBc).} \tag{2}$$

B. Data Extraction and Modeling

To extract the linear and distortion terms dependent on the power level, the baseband extraction setup has been configured, as shown in Fig. 6. The parameters of the main amplifier with 5-W PEP LDMOSFET can be directly extracted by monitoring the power spectral density (PSD) probed at the output load of the main amplifier with sweeping "**sweep 1**" depicted in Fig. 6 through an operating power level. The parameters for the error amplifier can be extracted by a little more sophisticated procedure. The pure error signal of the main amplifier is extracted from the signal-cancellation loop, and the signal is applied to the error amplifier as an input signal and to the error reference path to extract the distortion signal generated by the error amplifier. The "**control 1**" adjusts the gain of the variable gain amplifier (VGA) to obtain the signal at the power monitor with the minimum correlation between the reference and error signals, thereby to obtain the pure error signal from the main amplifier. To acquire the accurate parameters of the error amplifier, another cancellation loop is employed. The "**control 2**" functions in the same manner as "**control 1**" to extract the pure distortion signal from the error amplifier. "**sweep 1**" and "**sweep 2**" are simultaneously swept to obtain three-dimensional data, which are dependent on the signal power level of the main amplifier and spectrum emission level delivered to the error amplifier.

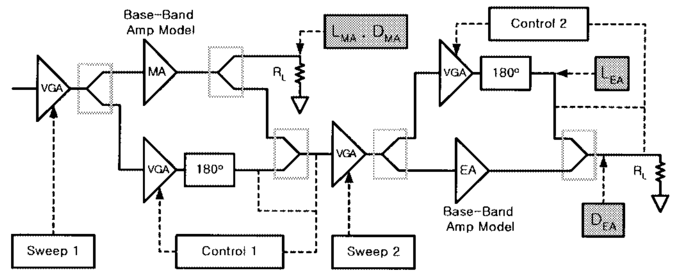

Fig. 6. Baseband data extraction setup for the linear and distortion terms dependent on the power level.

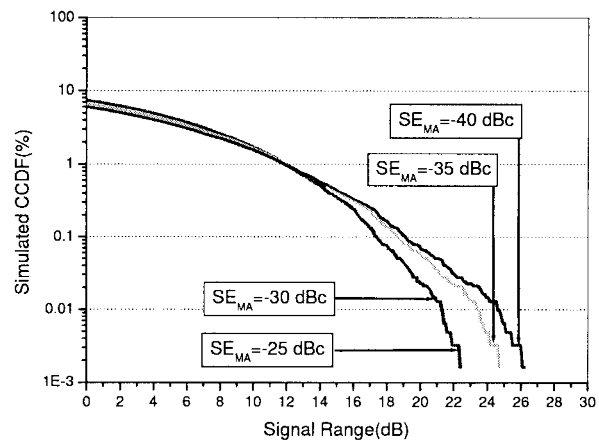

Fig. 7. CCDFs of the error signals according to the various spectrum emission levels of the main amplifier output.

The distortion generated by the error amplifier depends on the spectrum emission level of the main amplifier output, as well as the output power level of the error amplifier. The complementary cumulative probability density function (CCDF) of the error signals according to the various spectrum emission levels of the main amplifier output are plotted in Fig. 7. The peak-to-average ratios of the error signals reach around 20 dB at 0.1% point of the CCDF, although the peak-to-average ratio of the down-link WCDMA signal with 16 data channels is approximately 8.6 dB at the 0.1% point of the CCDF. The very high peak-to-average ratio of the error signal causes premature saturation of the error amplifier, which can be a source of extraordinarily high distortion.

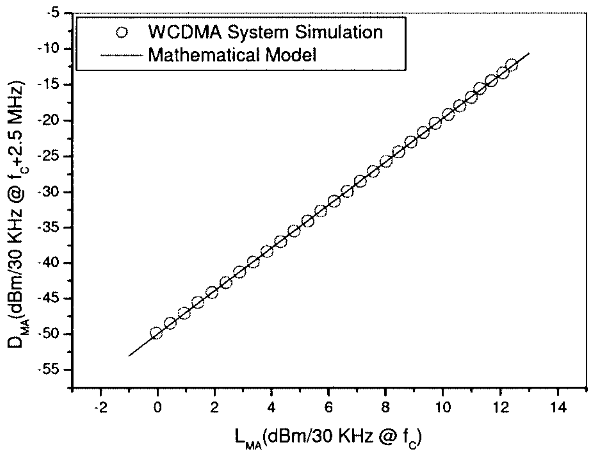

(a)

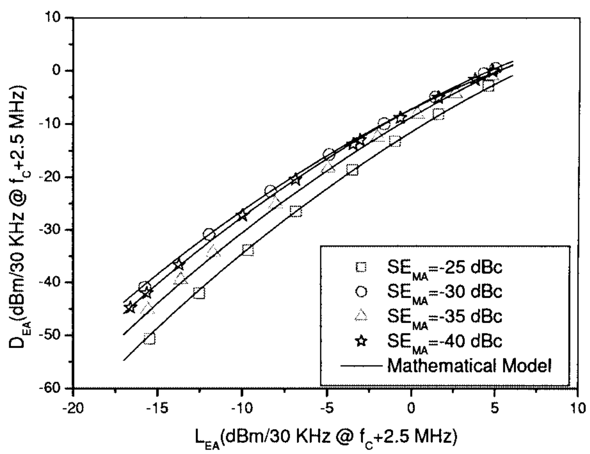

(b)

Fig. 8. Modeling results. (a) Extracted (scatter) and modeled (solid line) D_{MA}. (b) Extracted (scatter) and modeled (solid line) D_{EA}.

From the extracted data, the distortion terms of the main and error amplifiers are modeled using the simple polynomial expansion

$$D_{\mathrm{MA}} = f(L_{\mathrm{MA}}) = a_0 + a_1 L_{\mathrm{MA}} \text{ (dBm/30 kHz)} \qquad (3)$$

$$\begin{aligned} D_{\mathrm{EA}} &= f(L_{\mathrm{EA}}, \mathrm{SE}_{\mathrm{MA}}) \\ &= b_0 + b_1 L_{\mathrm{EA}} + b_2 L_{\mathrm{EA}}^2 + b_3 \mathrm{SE}_{\mathrm{MA}} + b_4 \mathrm{SE}_{\mathrm{MA}}^2 \\ &\quad + b_5 L_{\mathrm{EA}} \mathrm{SE}_{\mathrm{MA}} \text{ (dBm/30 kHz)}. \end{aligned} \qquad (4)$$

The distortion term of the main amplifier (D_{MA}) is modeled as a linear function of output power in the decibel scale (L_{MA}). The distortion term of the error amplifier (D_{EA}) is modeled as a second-order function of the error amplifier output (L_{EA}) and spectrum emission of the main amplifier ($\mathrm{SE}_{\mathrm{MA}}$) using multiple polynomial regression. The modeling results are shown in Fig. 8 [Fig. 8(a) shows the extracted (circles) and the modeled (solid line) D_{MA} and Fig. 8(b) shows the extracted (circle) and the modeled (solid line) D_{EA}]. The model parameters are presented in Table II.

III. Linearity Calculation

The optimization process using the mathematical model has many prior assumptions, most of which will be readdressed during the derivation of the equations. The reasonable assumptions used in this optimization process can be summarized as follows.

TABLE II
Modeled Parameters for the Distortion Terms of the Main and Error Amplifiers

param.	value	param.	value
a_0	-50.01	a_1	3.03
b_0	-48.84	b_1	2.213
b_2	-0.029	b_3	-2.645
b_4	-0.034	b_5	0.027

1) Signal cancellation at the first loop is perfectly performed.
2) The linear and distortion signals from the main or error amplifies are 100% uncorrelated.
3) There is no delay-line loss. Delay-line loss can be added, but the optimization routine is not changed.
4) There are no amplitude and phase mismatches at the error cancellation loop to purely investigate the effect on the distortion of the error amplifier.
5) Only the final stages of the main and error amplifiers are considered. Driver stages can be easily designed after determining the final stages of the main and error amplifiers.
6) The power capacity of the amplifiers is fixed using SR.
7) The output coupler has infinite directivity and no insertion loss.

The final output power and distortion level of the feedforward amplifier can be calculated using the mathematical model described in the previous section and the above assumptions. The second loop parameters, such as error amplifier size compared with that of the main amplifier and the coupling factor of the output coupler, are very important for linearization of the feedforward amplifier. Therefore, the total power from the main and error amplifiers is fixed to discover the optimum size ratio of the error and main amplifiers, i.e.,

$$PC_{\mathrm{MA}}(W) + PC_{\mathrm{EA}}(W) = PC_{\mathrm{TOTAL}}(W - PEP) \qquad (5)$$

where PC_{MA} and PC_{EA} are the power level of the main and error amplifiers, respectively. In this demonstration, the total power (PC_{TOTAL}) is fixed to 5 W. The size ratio between the error and main amplifiers is defined as

$$\mathrm{SR} = \frac{PC_{\mathrm{EA}}(W)}{PC_{\mathrm{MA}}(W)}. \qquad (6)$$

The calculation flow to optimize the second loop parameters for the linearization of the feedforward amplifier is visualized in Fig. 9. The flow for the linear signal of the main amplifier (L_{MA}), the flow for the distortion of the main amplifier (D_{MA}), which is identical to the linear term of the error amplifier (L_{EA}), and the flow for the distortion signal of the error amplifier (D_{EA}) are uncorrelated to each other and denoted using a solid, short, and long dashed line, respectively. The attenuators at the output of the main and error amplifiers are used to adjust the overall power level in (5) and the size ratio defined in (6). The output coupler is modeled as attenuators, which describe the coupling factor and coupling loss. The

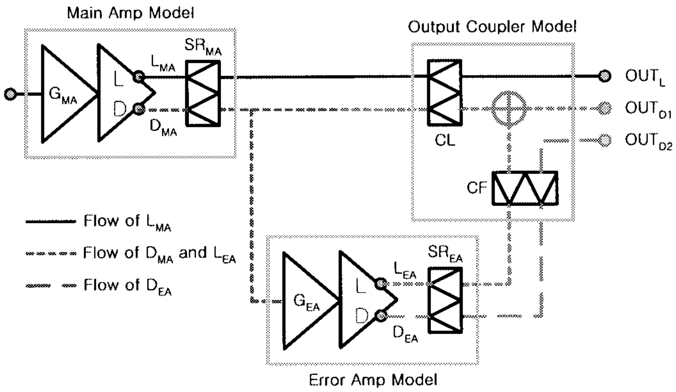

Fig. 9. Calculation flow to optimize the linearity of the feedforward amplifier.

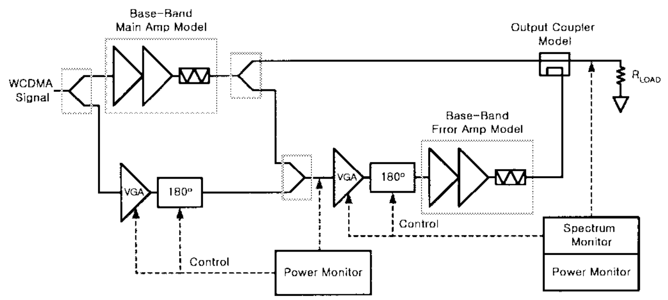

Fig. 10. Baseband WCDMA signal simulation setup for the feedforward amplifier.

delay-line loss can be easily inserted, but it is assumed to be zero in this calculation.

The output attenuation levels of the main and error amplifiers due to the definition of the size ratio (SR) become

$$\mathrm{SR}_{\mathrm{MA}} = -10\log\left(\frac{1}{1+\mathrm{SR}}\right)\ (\mathrm{dB}) \tag{7}$$

$$\mathrm{SR}_{\mathrm{EA}} = -10\log\left(\frac{\mathrm{SR}}{1+\mathrm{SR}}\right)\ (\mathrm{dB}). \tag{8}$$

The coupling loss (CL) dependent on the coupling factor (CF) is formulated in the decibel scale

$$\mathrm{CL} = -10\log\left(1-10^{(-CF)/10}\right)\ (\mathrm{dB}). \tag{9}$$

It is also assumed that the output coupler has infinite directivity and isolation properties.

The linearity of the feedforward amplifier can be calculated from the parameters of the linear output power level (OUT_L), size ratio (SR), and coupling factor (CF). Since the gain of the main amplifier (G_{MA}) does not have any effect on linearity, G_{MA} is not included in the formulation. However, the gain of the error amplifier (G_{EA}) is considered for the distortion cancellation. For perfect cancellation of the distortion term generated by the main amplifier, G_{EA} should be adjusted to

$$G_{\mathrm{EA}} = \mathrm{SR}_{\mathrm{EA}} - \mathrm{CL} + \mathrm{CF}\ (\mathrm{dB}) \tag{10}$$

with 180° phase difference.

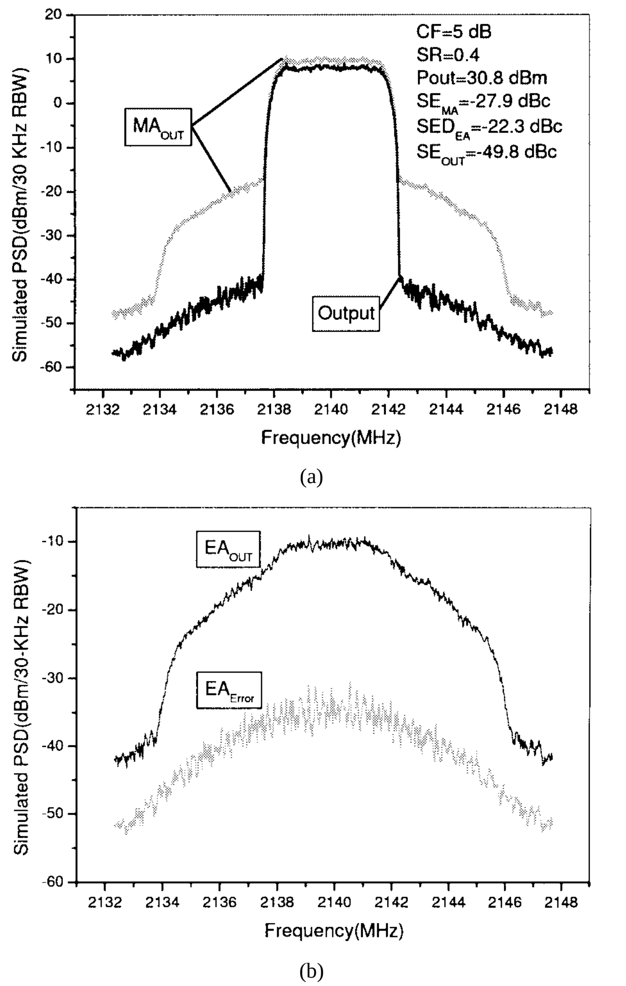

Fig. 11. Simulated PSDs. (a) Output signal of the main amplifier and the output signal after error cancellation to have 30.8 dBm of the channel average output power $\mathrm{CF} = 5$ dB and $\mathrm{SR} = 0.4$. (b) Amplified error signal and its distortion term extracted using the additional cancellation loop.

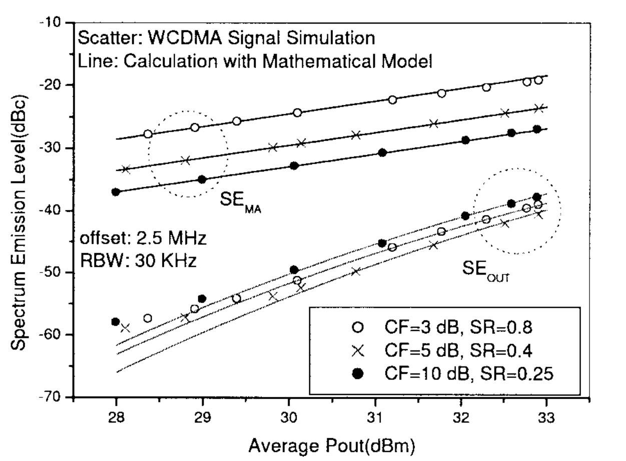

Fig. 12. Simulated spectrum emission level with the baseband WCDMA signal and the calculated results using the mathematical model.

The linear output signal of the main amplifier for the given final output power is given by

$$L_{\mathrm{MA}} = \mathrm{OUT}_L + \mathrm{SR}_{\mathrm{MA}} + \mathrm{CL}\ (\mathrm{dBm/30\ kHz}) \tag{11}$$

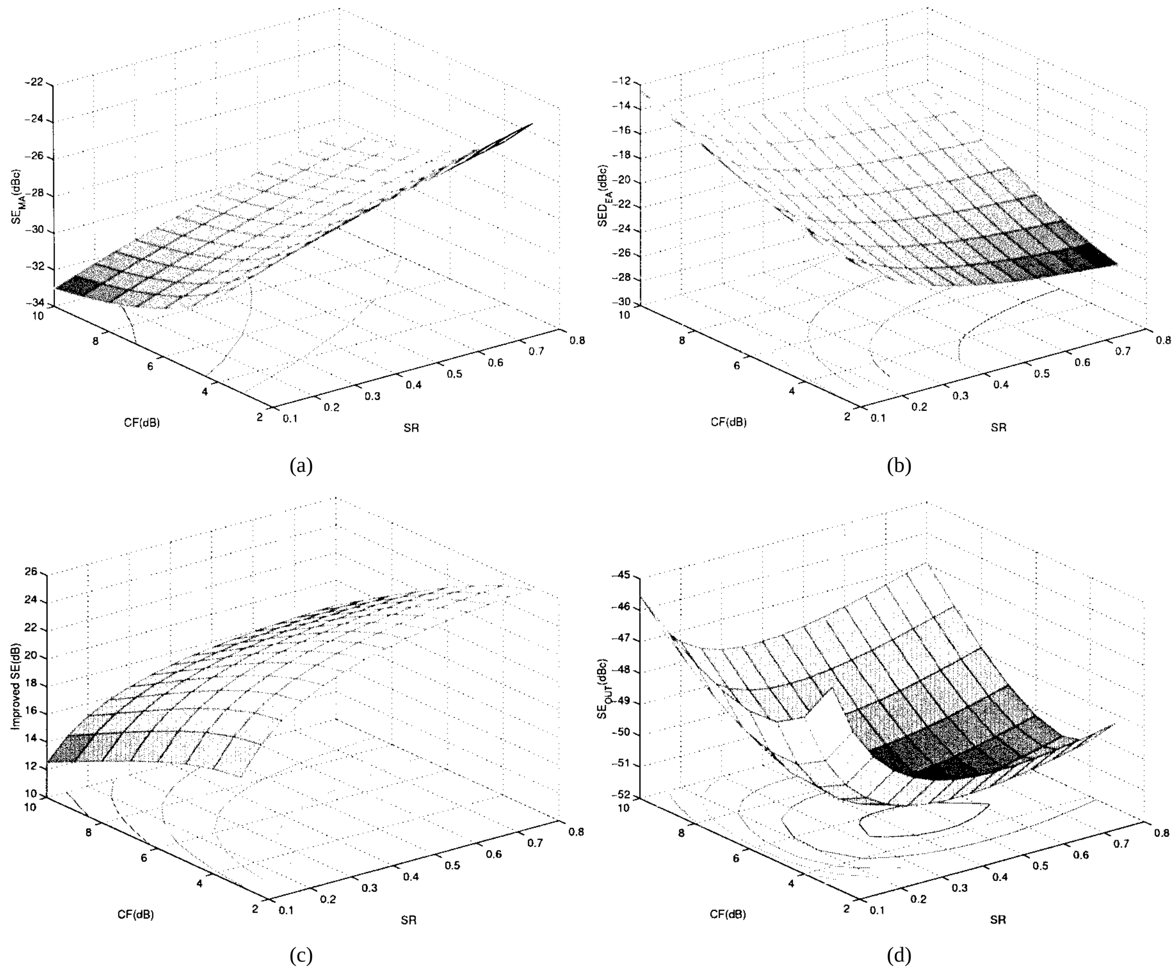

Fig. 13. (a) CF and SR dependent spectrum emission of the main amplifier. (b) Spectrum emission difference of the error amplifier. (c) Improvement of the output spectrum emission after cancellation. (d) Minimally achievable output spectrum emission level for a fixed channel output power of 30.5 dBm.

where OUT_L is the output spectral power at the center frequency with 30-kHz resolution bandwidth (RBW). The linear power of the error amplifier can be obtained as a function of L_{MA} from (11) as

$$L_{\mathrm{EA}} = D_{\mathrm{MA}}(L_{\mathrm{MA}}) - \mathrm{SR}_{\mathrm{MA}} + \mathrm{SR}_{\mathrm{EA}} - \mathrm{CL} + \mathrm{CF} \text{ (dBm/30 kHz)} \quad (12)$$

where $D_{\mathrm{MA}}(L_{\mathrm{EA}})$ can be computed using the mathematical model of (3).

The output distortion (OUT_{D2}) generated by the error amplifier can be determined from $D_{\mathrm{EA}}(L_{\mathrm{EA}}, \mathrm{SE}_{\mathrm{MA}})$ under the condition of the perfect cancellation of the distortion term generated by the main amplifier (i.e., $\mathrm{OUT}_{D1} = -\infty$)

$$\mathrm{OUT}_{D2} = D_{\mathrm{EA}}(L_{\mathrm{EA}}, \mathrm{SE}_{\mathrm{MA}}) - \mathrm{SR}_{\mathrm{EA}} - \mathrm{CF} \text{ (dBm/30 kHz)}. \quad (13)$$

The distortion term of the error amplifier $D_{\mathrm{EA}}(L_{\mathrm{EA}}, \mathrm{SE}_{\mathrm{MA}})$ can also be calculated using the mathematical model of (4) and definition of (1). Finally, the minimum spectrum emission of the output signal is given by

$$\mathrm{SE}_{\mathrm{OUT}} = \mathrm{OUT}_{D2} - \mathrm{OUT}_L \text{ (dBc)}. \quad (14)$$

The linearization properties of the feedforward amplifier can be investigated by evaluating (14) with sweeping parameters such as SR, CF, OUT_L, etc.

IV. Validation of Modeling and Discussion for the Results

To validate the calculated results using the mathematical model, the baseband WCDMA signal simulation of the feedforward amplifier was performed. The simulation setup diagram is shown in Fig. 10. For the simulation, the size fixing for the main and error amplifiers has been made the same way as the calculation for the mathematical model. The first loop is controlled to have minimum residual power, which can be approximated as a perfect signal cancellation. The second loop is controlled to have minimum spectral power at the 2.5-MHz offset.

Fig. 11(a) shows the simulated output PSDs of the main amplifier before attenuation for a power level fixing and after error cancellation. The channel average output power is 30.8 dBm with $\mathrm{CF} = 5$ dB and $\mathrm{SR} = 0.4$. The PSDs of the amplified error signal and its distortion term extracted using the additional cancellation loop are shown in Fig. 11(b). The spectrum emission at 2.5-MHz offset of the output signal becomes −49.8 dBc under these conditions. Fig. 12 shows the simulated spectrum emission at 2.5-MHz offset using the baseband WCDMA signal (scatter) and the calculated results using the mathematical model (line). The simulated and calculated results of the main amplifier and final output signal are in perfect agreement across a large output power level. The mismatches of the spectrum emissions near 60 dBc are caused by the noise level of the baseband WCDMA source signal, which is not a concern in the real experiments. This model is accurate enough for circuit optimization. Therefore, circuit optimization for linearization, the size ratio (SR), and coupling factor (CF) has been conducted using a mathematical model calculation with MATLAB. For the fixed channel output power of 30.5 dBm, the resulting spectrum emission of the main amplifier, spectrum emission difference of the error amplifier, improvement of the output spectrum emission after cancellation, and minimally achievable output spectrum emission level are presented in Fig. 13(a)–(d), respectively.

As the coupling factor increases and the size ratio decreases, the spectrum emission of the main amplifier is monotonically decreased and the spectrum emission difference of the error amplifier is increased [see Fig. 13(a) and (b)]. Therefore, the improvement for linearization is decreased, as shown in Fig. 13(c). These results were largely anticipated. However, the minimum achievable spectrum emission level clearly has an optimum point due to the relationship between the spectrum emission of the main amplifier and improvement for linearization. From Fig. 13(d), to achieve 30.5 dBm of the average channel output power with a fixed spectrum emission specification of -51 dBc, the possible ranges of the optimum SR and CF are 0.45 and 5.5 dB, respectively. These optimum values of SR and CF are quite different from those of the general feedforward amplifiers having around 0.25 and 8–13 dB of SR and CF, respectively. At the optimum point, the improvement of the spectrum emission level becomes obvious within 25 dB. Hence, it is a reasonable estimate that the dominant degradation mechanism of error cancellation in the feedforward amplifier is premature saturation of the error amplifier due to the high peak-to-average ratio (around 20 dB).

V. Summary and Conclusions

There are many advantages of the mathematical model proposed in this paper. Its most important advantage may be a fast calculation time. Calculation time for the results shown in Fig. 13 take less than a few seconds. Other advantages related to time are ease and flexibility of data collection and parameter change with just a few code modifications. This simple model provides very accurate simulation results and can be built using the measured data or data extracted from the baseband signal simulation.

Contrary to its many advantages, there are also some limitations in the mathematical model. This model can handle 100% correlated or uncorrelated signals only, and there is difficulty in using this model for parametric linearization such as predistortion. It is also very difficult to include cross-distortion terms to investigate complex nonlinear behaviors.

To conclude, a new mathematical model approach with linear and distortion paths based on the baseband WCDMA signal simulation has been proposed. With our mathematical model, the linearity of the feedforward amplifier has been maximized by optimizing the second-loop parameters. The calculated results show the optimum size ratio of the main and error amplifiers and the optimum coupling factor of the output coupler. The results also show that the premature saturation of the error amplifier can be a major degradation mechanism of error cancellation in the conventional feedforward amplifier. The optimized results and the design process will be very useful to systematically develop a feedforward amplifier, especially for systems that are designed to adopt the modulated signal with a complex signal statistics and a high peak-to-average ratio.

References

[1] G. Hanington, P. Chen, P. M. Asbeck, and L. E. Larson, "High-efficiency power amplifier using dynamic power-supply voltage for CDMA applications," *IEEE Trans. Microwave Theory Tech.*, vol. 47, pp. 1471–1476, Aug. 1999.

[2] J. S. Kenney and A. Leke, "Design considerations for multicarrier CDMA base station power amplifier," *Microwave J.*, vol. 42, no. 2, pp. 76–86, Feb. 1999.

[3] Y. Yang, Y. Kim, J. Yi, J. Nam, B. Kim, W. Kang, and S. Kim, "Digital controlled adaptive feedforward amplifier for IMT-2000 band," in *IEEE MTT-S Int. Microwave Symp. Dig.*, June 2000, pp. 1487–1490.

[4] J. K. Cavers, "Adaptation behavior of a feedforward amplifier linearizer," *IEEE Trans. Veh. Technol.*, vol. 44, Feb. 1996.

[5] E. E. Eid and F. M. Ghannouchi, "Adaptive nulling loop control for 1.7 GHz feedforward linearization systems," *IEEE Trans. Microwave Theory Tech.*, vol. 45, Jan. 1997.

[6] R. G. Meyer, R. Eschenbach, and W. M. Edgerley, "A wide-band feedforward amplifier," *IEEE J. Solid-State Circuits*, vol. SSC-9, pp. 422–428, Dec. 1974.

[7] P. B. Kenington, P. A. Warr, and R. J. Wilkinson, "Analysis of instability in feedforward loop," *Electron. Lett.*, vol. 33, no. 20, pp. 1669–1671, Sept. 1997.

[8] A. Katz, "SSPA linearization," *Microwave J.*, vol. 42, no. 4, pp. 22–44, 1999.

[9] S. Narahashi and T. Nojima, "Extremely low-distortion multi-carrier amplifier self-adjusting feedforward (SAFF) amplifier," in *Proc. IEEE Int. Communications Conf.*, 1991, pp. 1485–1490.

[10] R. J. Wilkinson and P. B. Kenington, "Specification of error amplifiers for use in feedforward transmitters," *Proc. Inst. Elect. Eng.*, pt. G, vol. 139, no. 4, pp. 477–480, Aug. 1992.

[11] C. L. Larose and F. M. Ghannouchi, "Optimization of feedfoward amplifier power efficiency on the basis of input power statistics," in *IEEE MTT-S Int. Microwave Symp. Dig.*, June 2000, pp. 1491–1494.

[12] K. Horiguchi, M. Nakayama, Y. Sakai, K. Totani, H. Senda, Y. Ikeda, and O. Ishida, "A high efficiency feedforward amplifier with a series diode linearizer for cellular base stations," in *IEEE MTT-S Int. Microwave Symp. Dig.*, May 2001, pp. 797–800.

[13] K. J. Parson and P. B. Kenington, "The efficiency of a feedforward amplifier with delay loss," *IEEE Trans. Veh. Technol.*, vol. 43, pp. 407–412, May 1994.

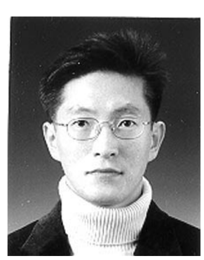

Youngoo Yang (S'99–M'02) was born in Hamyang, Korea, in 1969. He received the B.S. degree in electronic engineering from the Han-Yang University, Ansan, Korea, in 1997, and the Ph.D. degree in electrical and electronic engineering from the Pohang University of Science and Technology (POSTECH), Pohang, Korea, in 2002.

In 2002, he joined Skyworks Solutions Inc., Newbury Park, CA. His research interests include power-amplifier design, linearization techniques, efficiency-improving techniques, and modeling of high power amplifiers or devices.

Young Yun Woo was born in Taegu, Korea, in 1976. He received the B.S. degree in electronic and electrical engineering from the Han-Yang University, Seoul, Korea, in 2000, and is currently working toward the Ph.D. degree at the Pohang University of Science and Technology (POSTECH), Pohang, Korea.

His current research interests include RF power-amplifier design, linear power amplifier (LPA) system design, and baseband correction techniques for linearizing high power amplifiers.

Bumman Kim (S'77–M'78–SM'97) received the Ph.D. degree in electrical engineering from Carnegie-Mellon University, Pittsburgh, PA, in 1979.

From 1978 to 1981, he was engaged in fiber-optic network component research at GTE Laboratories Inc. In 1981, he joined the Central Research Laboratories, Texas Instruments Incorporated, where he was involved in development of GaAs power FETs and MMICs. He has developed a large-signal model of a power FET, dual-gate FETs for gain control, high-power distributed amplifiers, and various millimeter-wave MMICs. In 1989, he joined Pohang University of Science and Technology, Pohang, Korea, where he is a Professor in the Electronic and Electrical Engineering Department, and Director of the Microwave Application Research Center, where he works on device and circuit technology for MMICs. Currently, he is a Visiting Professor of Electrical Engineering at California Institute of Technology, Pasadena. He has authored more than 100 published technical papers.

Dr. Kim is a member of the Korean Academy of Science and Technology and Academy of Engineering of Korea.